

NOISE IN ELECTROPHYSIOLOGICAL MEASUREMENTS

In the most general sense, noise can be defined as any disturbance that interferes with the measurement of the desired signal. In electrophysiological measurements, such disturbances can arise from the preparation itself, the electrodes that couple the preparation to the measurement instrument, the electronic instrumentation (*e.g.*, voltage-clamp amplifier, patch-clamp amplifier), interference from external sources (*e.g.*, electrostatic and electromagnetic coupling between the circuitry and 50 or 60 Hz power lines, fluorescent lights, video monitors, and noise associated with mechanical vibrations), and, if the data is digitized (as is usually the case), from the digitization process itself (*e.g.*, quantizing noise, aliasing).

We will begin by discussing the basic noise mechanisms that arise from the physics of the materials and devices that comprise the electrical system. Interference from external sources and noise associated with digitization will be considered later.

The main fundamental types of noise are: thermal noise, shot noise, dielectric noise, and "excess" noise (*e.g.*, 1/f noise). These types of noise form the basis for a discussion of amplifier noise and electrode noise.

All the fundamental types of noise are completely random in nature. Their average properties can be measured, but their actual values at any particular instant in time cannot be predicted. The most convenient measure of the amplitude of noise is its root-mean-square (rms) value. Many noise processes have a Gaussian distribution of instantaneous amplitudes versus time. The area under the Gaussian distribution represents the probability that a noise event of a particular amplitude will occur (the total area is unity). The probability that a noise peak will exceed plus or minus one times its rms value is 0.32; the probability of a particular noise peak exceeding plus or minus three times its rms value is 0.003. It is common engineering practice to define peak-to-peak noise as 6 times the rms value; if the noise process has Gaussian distribution, the noise will remain within this bound 99.7% of the time. However, peak-to-peak noise is not as clearly defined as is rms noise, and it is not uncommon to find peak-to-peak noise operationally defined as anything from 5 times to 8 times rms.

When considering noise in the time domain, it is important to know the bandwidth over which the noise process is observed. Noise is made up of many frequency components, frequently extending from DC to many megahertz or gigahertz. Some noise processes are naturally



restricted in bandwidth, but most require the appropriate use of filtering to restrict the bandwidth of the noise while allowing adequate resolution of the signal. When a noise amplitude (rms or peak-to-peak) is discussed, it is appropriate to also note the bandwidth over which the noise is observed and the type of filter that has been used to restrict the bandwidth.

Due to the random nature of noise, uncorrelated noise sources will add in an rms fashion. Thus if E_1 , E_2 , and E_3 are the rms values of three uncorrelated noise sources, the total rms noise, E_T , of these sources together is given by:

$$E_T = \sqrt{E_1^2 + E_2^2 + E_3^2} \quad (1)$$

Because of this relationship, the largest individual source of noise will tend to dominate the total noise. For example, if two noise sources with rms values of 100 μV and 20 μV are added together, the resulting noise will have an amplitude of $\{(100 \mu\text{V})^2 + (20 \mu\text{V})^2\}^{1/2} = 102 \mu\text{V}$ rms.

Thermal Noise

Thermal noise results from random motion of thermally excited charge carriers in a conductor. It is often referred to as *Johnson noise* or *Nyquist noise*. For a resistor, thermal noise can be represented as a series voltage noise source or a parallel current noise source as illustrated in Figure 12-1. These two representations are equivalent.

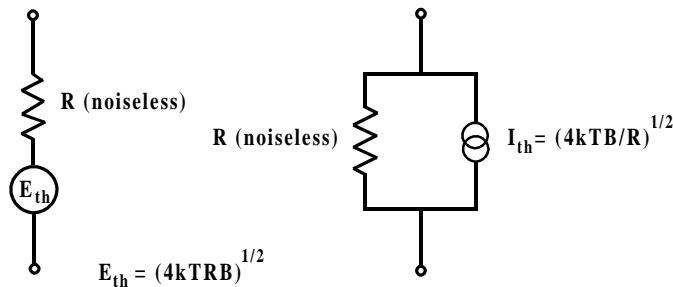


Figure 12-1. Noise Equivalent Circuits of a Resistor

The power spectral density (PSD) of thermal noise is white, *i.e.*, it does not vary with frequency. Its value, S_{thV}^2 , is given as a voltage noise by:

$$S_{thV}^2 = 4kTR \quad (\text{units: Volt}^2/\text{Hz}) \quad (2)$$

or, equivalently, as a current noise PSD, S_{thI}^2 , by:

$$S_{thI}^2 = \frac{4kT}{R} \quad (\text{units: Amp}^2/\text{Hz}) \quad (3)$$

where k is Boltzmann's Constant ($1.38 \times 10^{-23} \text{ J}/^\circ\text{K}$), T is the absolute temperature in degrees Kelvin ($^\circ\text{K} = ^\circ\text{C} + 273$), and R is the resistance in ohms. It should be noted that spectral densities are also often expressed in units of Volt/ $\sqrt{\text{Hz}}$ and Amp/ $\sqrt{\text{Hz}}$.



The variance (also called the noise power) over a bandwidth B (units: Hz) is then:

$$E_{th}^2 = 4kTRB \quad (\text{units: Volt}^2) \quad (4)$$

or

$$I_{th}^2 = \frac{4kTB}{R} \quad (\text{units: Amp}^2) \quad (5)$$

The rms noise over a bandwidth B is given by:

$$E_{th} = \sqrt{4kTRB} \quad (\text{units: Volt rms}) \quad (6)$$

or

$$I_{th} = \sqrt{\frac{4kTB}{R}} \quad (\text{units: Amp rms}) \quad (7)$$

Spectral densities, rms current and voltage noise for bandwidths of 1 and 10 kHz are listed in Table 12-1 for resistances of 100 Ω to 100 GΩ. Note that while thermal voltage noise increases with increasing resistance, thermal current noise decreases as the resistor's value increases.

Value	1 kHz V noise (μV rms)	10 kHz V noise (μV rms)	1 kHz I noise (pA rms)	10 kHz I noise (pA rms)	Voltage Density (nV/√Hz)	Current Density (pA/√Hz)
100 Ω	0.040	0.126	400	1260	1.26	12.6
1 kΩ	0.126	0.40	126	400	4.0	4.0
10 kΩ	0.4	1.26	40	126	12.6	1.26
100 kΩ	1.26	4.0	12.6	40	40	0.4
1 MΩ	4.0	12.6	4.0	12.6	126	0.126
10 MΩ	12.6	40	1.26	4.0	400	0.040
100 MΩ	40	126	0.40	1.26	1260	0.0126
1 GΩ	126	400	0.126	0.40	4000	0.004
10 GΩ	400	1260	0.040	0.126	12600	0.0013
100 GΩ	1260	4000	0.013	0.040	40000	0.0004

Table 12-1. Thermal Noise of Resistors

Shot Noise

Shot noise arises when current flows across a potential barrier, *e.g.*, a *p-n* junction in a semiconductor device. Since potential barriers are not present in simple resistive elements, resistors do not display shot noise. Over a bandwidth B, the rms value of the shot noise current is given by:



$$I_{\text{sh}} = \sqrt{2qIB} \quad (\text{units: Amp rms}) \quad (8)$$

where q is the charge of the elementary charge carrier (for electrons $q = 1.6 \times 10^{-19}$ coulomb) and I is the DC current in Amps.

An important example of shot noise is the equivalent input current noise of an operational amplifier that arises from its input bias current I_b (also referred to as gate current for FET¹ input devices). For bipolar transistor input devices, I_b is typically in the range of 1 nA to 1 μ A; for FET input operational amplifiers, I_b (at room temperature) is typically in the range of 1 to 10 pA, and can be less than 0.5 pA for special devices. The rms value of shot noise for operational amplifiers with I_b ranging from 0.1 pA to 1 μ A in a 1 and 10 kHz bandwidth are listed in Table 12-2. In capacitive-feedback patch voltage-clamp amplifiers (*e.g.*, the Axopatch 200 series), shot noise current from the headstage amplifier sets the noise floor at low-to-moderate frequencies. By design these devices display very low levels of shot noise; selected units can have gate currents as low as 0.2 pA, resulting in low-frequency current noise less than that of a 250 G Ω resistor.

Op Amp Bias Current	1 kHz Shot Noise (pA rms)	10 kHz Shot Noise (pA rms)
1 μ A	18	57
100 nA	5.7	18
10 nA	1.8	5.7
1 nA	0.57	1.8
100 pA	0.18	0.57
10 pA	0.057	0.18
1 pA	0.018	0.057
0.1 pA	0.0057	0.018

Table 12-2. Shot Noise

Dielectric Noise

An ideal lossless capacitor does not produce thermal noise. However, all real dielectric materials display some loss that results in the generation of thermal noise. For dielectrics with relatively low losses, the spectral density of this noise S_D^2 can be described in terms of the dissipation factor D and the capacitance C_D of the dielectric:

$$S_D^2 = 4kTDC_D(2\pi f) \quad (\text{units: Amp}^2/\text{Hz}) \quad (9)$$

Where f is the frequency in Hz. The PSD of dielectric noise characteristically rises linearly with increasing frequency. The dissipation factor is often listed as $\tan \delta_e$ where δ_e is the loss angle (note that for small δ_e , $\tan \delta_e \approx \delta_e$); the "quality factor" Q is the inverse of D ($Q = 1/D$). For a bandwidth extending from DC to an uppermost cut-off frequency B , the rms noise current I_D , resulting from a lossy dielectric, is given by:

¹FET is Field Effect Transistor



$$I_D = \sqrt{4kTDC_D\pi B^2} \quad (\text{units: Amp rms}) \quad (10)$$

For the best solid dielectrics (*e.g.*, quartz, sapphire and some ceramics), D is on the order of 10^{-5} to 10^{-4} . For poorer (lossier) dielectrics D can be much higher; *e.g.*, some thermosetting plastics have D in the range of 0.01 to 0.1. For some glasses used to fabricate patch pipettes, D is at least 0.01. The dissipation factor has some frequency dependence, although in the important range from about 1 kHz to 100 kHz it is usually reasonable to approximate it as a constant. D also shows some temperature dependence (typically decreasing with lower temperatures), although again in the usual range of temperatures it may be considered constant.

Dielectric noise is one consideration in the selection of feedback and compensation capacitors in capacitive-feedback headstages for patch clamping. It must also be considered in the packaging materials, electrode holders, etc. for any high-sensitivity current or charge amplification device. By using high-quality capacitors ($D \leq 0.0001$) the dielectric noise of the feedback and compensation capacitor can be made a relatively insignificant component of the total noise of present day capacitive-feedback headstages. For example, using equation (10) it can be estimated that for $D = 0.0001$ and $C_D = 2$ pF (1 pF feedback capacitor and 1 pF compensation capacitor), the dielectric noise of these components in a 10 kHz bandwidth is only about 0.032 pA rms. Dielectric noise associated with packaging (*i.e.*, with the input gate lead of the patch-clamp headstage) can be somewhat higher. The most important source of dielectric noise in common electrophysiological measurements is the dielectric noise of the glass used to fabricate pipettes for patch voltage clamping. This subject will be considered in greater detail below (see **Electrode Noise**). It is worth noting that a dielectric does not actually have to be in contact with the input of a sensitive current amplifier, such as a patch-clamp headstage, in order to produce noise. For example, a 1 pF capacitor formed by a high-loss dielectric with $D = 0.1$ that is coupled *through air* to the input by a capacitance of 1 pF can result in approximately 0.35 pA rms in a 10 kHz bandwidth. Thus it is a good idea both in the design of headstage electronics and of an experimental patch clamp set-up not to have exposed, high-loss dielectrics in the immediate vicinity of the input.

Excess Noise

Excess noise can broadly be defined as any noise that is present in a circuit element in addition to the fundamental noise mechanisms already described. For example, in the presence of direct current all resistors exhibit low-frequency noise whose power spectral density varies inversely with frequency. This noise is present in addition to the thermal noise of the resistor and is usually referred to as "1/f noise." Different resistor types display different amounts of 1/f noise, with metal film and wirewound types showing the least excess low-frequency noise and carbon composition resistors showing the most. The PSD (in V^2/Hz) of this excess noise rises with decreasing frequency essentially as 1/f. Its magnitude is directly proportional to the DC current flowing through the resistor. Semiconductor devices also exhibit 1/f noise.

High-value (gigohm range) resistors, such as those used as the feedback element in resistive-feedback patch-clamp headstages, also display a form of excess noise that rises with increasing frequency. Generally, such resistors only achieve their thermal noise level (which is the minimum possible) in the frequency range from about 10 Hz to 1 kHz. At low frequencies, 1/f



noise is observed, and at high frequencies the noise PSD typically rises as f^α , where α is usually in the range of 1 to 2. This noise can result in rms noise from a resistor having several times the predicted thermal noise value in a 10 kHz bandwidth. The elimination of this noise source is one of the motivations behind using capacitive-feedback in patch clamps such as the Axopatch 200 series.

Amplifier Noise

The intrinsic noise of an operational amplifier can be described by an equivalent input voltage noise E_n in series with the negative (-) input and an equivalent input current noise I_n between the positive (+) and negative (-) inputs (see Figure 12-2). These noise sources have been referred to the input for convenience of analysis. It should be noted, however, that they are measured at the output. For example, in an open-loop situation (such as shown in Figure 12-2), if the inputs are grounded, the voltage at the negative (-) input will be zero (ground). E_n must be inferred by measuring the output noise voltage and dividing it by the open-loop gain (both are frequency dependent) of the amplifier. On the other hand, in a closed-loop situation (which is always the case when using operational amplifiers, as illustrated in Figure 12-3), E_n will actually appear at the negative (-) input due to the action of the feedback loop.

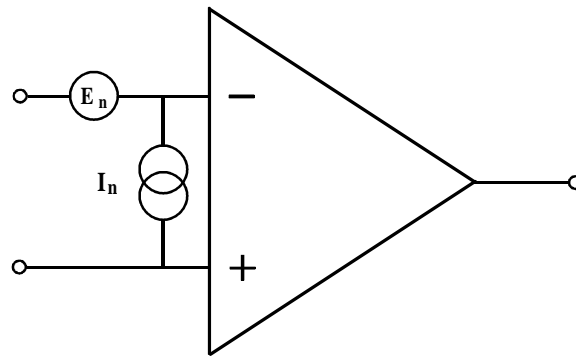


Figure 12-2. Operational Amplifier Noise Model

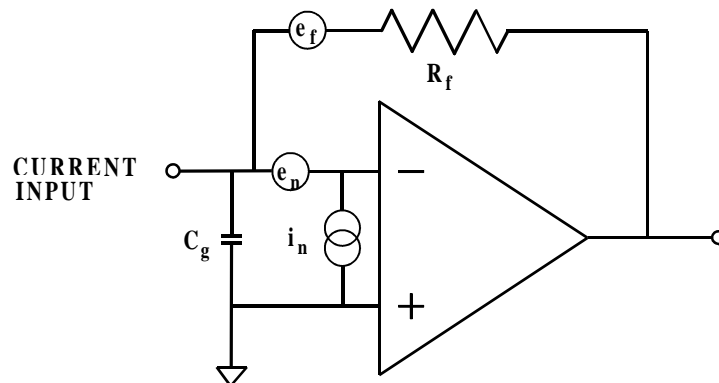


Figure 12-3. Noise Model of a Simplifier Current-to-Voltage Converter



When analyzing the noise of an operational circuit it is convenient to consider the noise sources in terms of their power spectral densities. In this case the noise sources will be denoted by lower case symbols, *e.g.*, $e_n(f)$ (units: $V/\sqrt{\text{Hz}}$) or $e_n^2(f)$ (units: V^2/Hz). As a useful example of noise analysis in an operational circuit, consider the simplified current-to-voltage converter illustrated in Figure 12.3. In this circuit e_n and i_n are the input voltage and current noise PSDs, respectively, and e_f is the PSD of the noise (thermal and excess) of the feedback resistor R_f . The current to be measured is introduced at the terminal labeled "input." For simplicity, the positive (+) input is shown to be grounded. C_g is any capacitance between the negative (-) input and ground; this includes the input capacitance of the amplifier plus strays and is usually about 15 pF. The noise PSD at the output of the IV converter, $S_{\text{out}}^2(f)$, can be shown to be:

$$S_{\text{out}}^2(f) = i_n^2 R_f^2 + e_f^2 + e_n^2 (1 + 4\pi^2 f^2 R_f^2 C_g^2) \quad (\text{units: } V^2/\text{Hz}) \quad (11)$$

It is useful to present this result in terms of current so it can be compared directly with the current signal being measured. This is accomplished by dividing the above expression by R_f^2 , thus referring the noise to the input. The input referred PSD, $S_{\text{in}}^2(f)$, is then given by:

$$S_{\text{in}}^2(f) = i_n^2 + \frac{e_f^2}{R_f^2} + e_n^2 \left(\frac{1}{R_f^2} + 4\pi^2 f^2 C_g^2 \right) \quad (\text{units: } \text{Amp}^2/\text{Hz}) \quad (12)$$

In general, i_n , e_n and e_f are all functions of frequency: i_n is the shot noise of the input gate current of the amplifier but usually displays some 1/f behavior at low frequencies; e_f is the thermal and excess noise of R_f ; and e_n also displays 1/f behavior at low-to-moderate frequencies. Nevertheless, it is convenient to assume that each of these terms is independent of frequency so that equation (12) can be easily integrated over a frequency band (for instance, DC to some uppermost bandwidth denoted by B). The square root of this result is then the rms noise for the bandwidth B:

$$I_{\text{in}} = \sqrt{i_n^2 B + \frac{e_f^2}{R_f^2} B + e_n^2 \frac{B}{R_f^2} + \frac{4}{3} \pi^2 C_g^2 B^3} \quad (13)$$

It should be noted that if it is assumed that e_f is only the thermal noise of the feedback resistor, then the term e_f^2/R_f^2 is simply $4kT/R_f$ (see equation (3) above).

It is instructive to consider the relative magnitudes of the various terms in equation (12) or (13). In the case of a patch voltage clamp, the value of R_f is selected to be very high, both to provide adequate gain to resolve tiny (pA) currents and to minimize the noise contribution of this resistor; 50 G Ω is common for single-channel recording. The PSD of the thermal noise of an ideal 50 G Ω resistor is 3.2×10^{-31} Amp^2/Hz and the rms noise associated with such a component over a bandwidth of 10 kHz is 0.057 pA rms (although as already noted, excess high-frequency noise can increase this value several fold). The shot noise, which accounts for i_n , associated with an input gate current of 0.2 pA would, by itself, produce noise of about 0.025 pA rms in a 10 kHz bandwidth. For a typical high-quality patch-clamp headstage, e_n is about 2-3 nV/ $\sqrt{\text{Hz}}$ at frequencies above about 1 kHz; C_g is usually about 15 -20 pF. With these values, the term $(\frac{4}{3} \pi^2 e_n^2 C_g^2 B^3)^{1/2}$ amounts to roughly 0.15 pA rms in a 10 kHz bandwidth. These three terms should be uncorrelated; therefore, they sum in an rms fashion so that the total predicted noise is



$(0.057^2 + 0.025^2 + 0.15^2)^{1/2} = 0.162$ pA rms. For a resistive-feedback headstage, actual noise in a 10 kHz bandwidth is normally substantially higher (about 0.25 -0.30 pA rms) both because of excess noise from the feedback resistor and because of the characteristics of the low-pass filters that do not abruptly cut off noise at the -3dB bandwidth (see below). Nevertheless, it is important to note that for bandwidths above a few kilohertz, the term arising from e_n and C_g dominates total noise. To intuitively understand the origin of this term, it is only required to remember that the current through a capacitor is directly proportional to the rate of change of voltage across the capacitor ($I = C(dV/dt)$). Therefore, the voltage noise at the negative (-) input of the amplifier produces current noise through the capacitor C_g . This noise increases with increasing frequency simply because higher frequency components of the voltage noise involve more rapidly changing voltages. The noise current through the capacitor is supplied by the feedback resistor and therefore appears as noise at the amplifier output.

Electrode Noise

Noise associated with recording electrodes is significant and often dominant in most electrophysiological measurements. In microelectrode voltage clamps and the whole-cell variant of the patch voltage-clamp technique, the thermal voltage noise of the electrode is of greatest importance since this noise will exist across the cell membrane and produce large levels of current noise in conjunction with the membrane capacitance. In patch single-channel measurements using the patch clamp, the voltage noise of the electrode is also important; but here the situation is further complicated by such factors as the dielectric noise of the pipette that produces a major source to overall noise. We will consider noise associated with the electrode in single-channel recording and whole-cell patch recording separately, beginning with the single-channel recording.

Electrode Noise in Single-Channel Patch Voltage Clamping

There are a variety of mechanisms by which the patch pipette contributes noise to the measured current in the patch voltage-clamp technique. The first mechanism we will consider here is the fact that the holder plus pipette add a significant amount of capacitance to the headstage input. This capacitance reacts with the input voltage noise, e_n , of the headstage amplifier to produce current noise with a PSD that rises with frequency in essentially the same fashion as the PSD of the open-circuit headstage. In fact, this noise is perfectly correlated with the noise resulting from the intrinsic capacitance, C_{in} , associated with the headstage input. Note that C_{in} consists of the input capacitance of the JFET ($C_{iss} = C_{gs} + C_{gd}$, where C_{gs} is the gate-source capacitance and C_{gd} is the gate-drain capacitance), plus any compensation capacitors connected to the input, plus, for a capacitive-feedback headstage, the feedback capacitor (1 pF for the Axopatch 200) and capacitance associated with the reset switch, plus about 1-2 pF of stray capacitance: in total, C_{in} is usually about 15 pF. Denoting the holder plus electrode capacitance as C_{he} , the PSD of the current noise arising from e_n is given by $4\pi^2 e_n^2 (C_{in} + C_{he}) f^2$. The capacitance of the holder can vary from about 1-5 pF; larger capacitances are associated with holders with metallic shielding. The pipette capacitance depends on the depth of immersion of the pipette, the type of glass used, the thickness of the pipette wall, and the use of Sylgard coating. The total capacitance of the pipette will generally be in the range of 1-5 pF. Thus, C_{he} can range from 2-10 pF. With $C_{he} = 2$ pF, the increment in wideband noise from this mechanism above that of the open-circuited headstage should not be much more than 10%. However, with $C_{he} = 10$ pF the noise



increment could be more than 50% from this mechanism alone. Obviously, from the point of view of noise, it is important to minimize the capacitance of the holder and pipette.

Dielectric Noise

The basic characteristics of dielectric noise have already been described above (see equations (9) and (10)). Dielectric noise of the pipette can be a major contributor to total noise in patch voltage clamping; in some situations it can be the dominant noise source. The dielectric noise arising from the pipette depends on the dissipation factor D of the glass used to fabricate the pipette, on the pipette capacitance (C_D in equations (9) and (10)), and on the presence of Sylgard coating. The dissipation factor D of glasses other than quartz that have been successfully used for patch pipettes generally falls in the ranges of 0.001-0.01. The dissipation factor for quartz is variously reported to be 10^{-5} to as much as 4×10^{-4} . For Amersil T-08 quartz, which has been used in all of the preliminary tests of quartz pipettes described below, the reported dissipation factor is 10^{-4} . For uncoated pipettes the value of C_D is determined by the dielectric constant ϵ of the glass, the ratio of the outer diameter (OD) to the inner diameter (ID) of the pipette, the depth of immersion of the pipette into the bath, and to some extent by the pulling characteristics of the glass and the geometry near its tip. The dielectric constant ϵ ranges from as little as 3.8 for quartz to more than 9 for some high-lead glasses. Typical glass capillaries used in the fabrication of patch pipettes have an OD of 1.65 mm and an ID of 1.15 mm; thus $OD/ID \approx 1.43$. If it is assumed that these proportions ($OD/ID = 1.43$) are maintained as the glass is drawn out in pulling, then for uncoated pipettes the value of C_D will be approximately 0.15ϵ pF per mm of immersion into the bath. For thick-walled glass with $OD/ID = 2$, this value would fall to 0.08ϵ pF per mm of immersion; while for thin-walled glass with $OD/ID = 1.2$ the capacitance would increase to about 0.30ϵ pF per mm.

Actual measurements with uncoated or lightly Sylgard-coated pipettes fabricated from glasses with known ϵ and immersed to a depth of 2-3 mm indicate that these values often underestimate pipette capacitance; therefore, the dielectric noise is also underestimated. This is probably due to non-uniform thinning near the tip and to some uncertainty as to the true depth of immersion (due to a meniscus of solution around the pipette). For example, using the popular Corning 7052 glass, which has $\epsilon = 4.9$ and with $OD/ID \approx 1.43$, it is not uncommon to measure a pipette capacitance as high as ≈ 3 pF, *i.e.*, about twice the predicted value, when an uncoated pipette or a pipette very lightly coated with Sylgard is immersed at a depth of 2 mm.

Despite this precautionary note, it is clear that, all else being equal, the value of C_D varies linearly with the dielectric constant ϵ of the glass. Equation (10) indicates that if the depth of immersion and the OD/ID ratio are constant, the rms noise for a given bandwidth arising from the lossy dielectric characteristics of pipettes fabricated from various glasses will be proportional to $(D\epsilon)^{1/2}$. Thus the lowest noise glasses are expected to be those that minimize the product of the dissipation factor and the dielectric constant. This relationship has been born out experimentally in tests of some 20 different types of glass used to fabricate patch pipettes (Rae and Levis, Personal Communication).

To illustrate the range of results expected for different glass types, we will consider three pipettes with identical geometry fabricated from three different glasses. It will be assumed that $OD/ID \approx 1.4$, $C_D = 0.2\epsilon$ pF per mm of immersion, the immersion depth is 2 mm, the



pipettes are uncoated or are coated very lightly with Sylgard (so that the coating does not reduce the dielectric noise significantly), and the rms noise is measured at a 10 kHz bandwidth (-3 dB, 8-pole Bessel filter). Corning 7052 glass ($D \approx 0.003$ and $\epsilon \approx 5$) represents reasonably low-loss glasses used to fabricate patch pipettes. Under the above stated conditions, the C_D value of this pipette is 2 pF and the dielectric noise contribution predicted by equation 10 is about 0.17 pA rms, or about 0.2 pA rms if the characteristics of an 8-pole Bessel filter are taken into account. On the other hand, 0080 soda lime glass ($D \approx 0.01$, $\epsilon \approx 7$) represents high-loss glasses, which were commonly used in the early days of patch clamping. Its $C_D = 2.8$ pF and dielectric noise of about 0.44 pA rms is predicted. Finally, Corning 7760 is a very low-loss glass with $D \approx 0.0017$ and $\epsilon \approx 4.5$. With $C_D = 1.8$ pF, a dielectric noise of slightly less than 0.15 pA rms is predicted. These figures are in reasonable agreement with experimental findings that have attempted to separate the components of total noise arising from the dielectric noise of pipettes fabricated from various glasses.

Since the capacitance C_D increases approximately linearly with increasing depth of immersion, the dielectric noise for any particular type of glass and OD/ID ratio should vary approximately as the square root of the depth immersion. From the point of view of noise reduction, it is clearly useful with excised patches to withdraw the pipette tip as close to the surface of the bath as possible. If the patch cannot be excised, then the bath should be as shallow as possible. For example, for a pipette fabricated from Corning 7760, as in the previous example, dielectric noise is expected to decrease from about 0.15 pA rms in a 10 kHz bandwidth for a 2 mm immersion depth to roughly 0.05 pA rms for a 0.2 mm immersion depth. The effect of immersion depth on pipette noise has, at least qualitatively, been verified experimentally. A method employing Silicone fluid to minimize the effective pipette immersion depth was introduced by Rae and Levis (1992) and is described below.

The above discussion dealt with expected behavior for uncoated pipettes. However, it is common practice (and highly recommended for low-noise measurements) to apply a coating of Sylgard #184 covering the entire tapered region of the pipettes (*i.e.*, approx. 5 - 10 mm) and extending to within roughly 100 μm of the tip (see **Chapter 4**). Coating with a hydrophobic substance such as Sylgard is necessary to prevent the formation of a thin film of solution that will creep up the outer wall of an uncoated pipette. Such a film can produce very large amounts of noise in uncoated pipettes. Sylgard coating not only virtually eliminates this noise source but also thickens the wall of the pipette thereby reducing its capacitance. The dielectric constant of Sylgard #184 is 2.9 and its dissipation factor is ≈ 0.002 , which is lower than that of most glasses that have been used for patch pipette fabrication. Thus, coating with Sylgard will reduce dielectric noise of patch pipettes. It is expected that the improvement in noise associated with Sylgard coating will be greatest for glasses with a high $D\epsilon$ product (*e.g.*, soda lime glass); this has been confirmed experimentally. Improvement of noise should be less for glasses with very low values of $D\epsilon$, but coating with Sylgard will reduce the dielectric noise of all glasses. The effects of Sylgard coating on noise are, however, difficult to quantify theoretically primarily because the thickness of the coating is usually not uniform. In particular, it is difficult to achieve a very thick coating very near the tip.

Experimental tests of the noise properties of patch pipettes fabricated from 19 different kinds of glass (see **Chapter 4**) have confirmed the general conclusions described above.



With few exceptions, the noise attributable to the pipette is inversely correlated with the $D\epsilon$ product of the glass. In addition, thicker-walled pipettes and shallow depths of immersion reduce noise for any particular glass type. Sylgard coating has its greatest effect on the glasses with the poorest inherent electrical properties, but it is important to remember that such coating is necessary *for all types of glass*.

It has been obvious for some time that pipettes fabricated from quartz should produce only very small amounts of dielectric noise due to the low dielectric constant of quartz ($\epsilon = 3.8$) and, more importantly, its extremely low dissipation factor ($D \approx 10^{-5} - 10^{-4}$). However, due to the high melting point of quartz ($\approx 1600^\circ\text{C}$), it has only recently become practical to pull patch pipettes from quartz tubing. A quartz pipette with $D = 10^{-4}$ that is immersed to a depth of 2 mm (again assuming 0.2ϵ pF per mm of immersion) would be predicted to produce only about 0.03 pA rms of dielectric noise in a bandwidth of 10 kHz (-3 dB, 8-pole Bessel filter); for $D = 10^{-5}$ this value would fall to 0.01 pA rms. Preliminary measurements using Amersil T-08 quartz suggest that the amount of dielectric noise in this situation is closer to 0.04-0.05 pA rms. A more detailed discussion of preliminary estimates of the noise properties of quartz pipettes is provided below.

Dielectric noise is probably the largest source of noise for pipettes fabricated from all glasses other than quartz. For pipettes fabricated from quartz, due to its very low dissipation factor sources of noise other than dielectric noise are expected to dominate total pipette noise (see below).

To summarize, dielectric noise can be minimized by using thick-walled glasses with low values of $D\epsilon$ and coating the pipette with Sylgard #184. The effects of Sylgard coating are greatest for glasses with relatively poor electrical properties. For excised patches, dielectric noise can be minimized by withdrawing the tip of the pipette as close as possible to the surface of the bath.

It should be noted that dielectric noise will also contribute to the noise associated with the holder. For an Axopatch 200A with an open circuit noise of 0.06 pA rms in a 5 kHz bandwidth, total noise should not increase to more than about 0.07 pA rms in this bandwidth when the Axon-supplied polycarbonate holder is attached. Part of this noise increment is due to the fact that the holder adds about 1 - 1.5 pF of capacitance to the headstage input. The rest of the increment in noise associated with the holder is presumably dielectric noise, which can be estimated to account for roughly 0.03 pA rms in a 5 kHz bandwidth.

Noise Arising From Distributed Pipette Resistance and Capacitance

Most of the resistance of a patch pipette resides at or very near its tip. On the other hand, the capacitance of an uncoated pipette can be expected to vary linearly with its depth of immersion into the bath. Therefore, it has sometimes been assumed that current noise arising from the thermal voltage noise of the pipette resistance in conjunction with the pipette capacitance can be assumed to be negligible in comparison with other noise sources. However, significant resistance resides in regions of the pipette that are further removed from the tip. The thermal voltage noise of this resistance will greatly exceed the input voltage noise of the headstage itself, with which it is in series. The actual situation is complicated because both the pipette resistance and capacitance are distributed. In this



section we will consider the pipette capacitance to be lossless, and initially the effects of Sylgard coating will not be considered. In order to estimate the noise arising from the distributed pipette resistance and capacitance, we will consider rather idealized pipette geometry.

The pipette has been modeled as a shank and a conical region approaching the tip; the angle of the cone is 11.4° and the tip opening is $1\ \mu\text{m}$ in diameter. With this cone angle the ID of the pipette increases to $100\ \mu\text{m}$ at a distance of $0.5\ \text{mm}$ from the tip, $200\ \mu\text{m}$ at a distance of $1\ \text{mm}$ from the tip, $300\ \mu\text{m}$ at a distance $1.5\ \text{mm}$ from the tip, etc. When filled with a solution with a resistivity of $50\ \Omega\text{cm}$ the pipette will have a total resistance of about $3.2\ \text{M}\Omega$. About $2.1\ \text{M}\Omega$ of this total resistance resides in the first $10\ \mu\text{m}$ from the tip; slightly more than $3\ \text{M}\Omega$ occurs in the first $100\ \mu\text{m}$ from the tip. However, about $80\ \text{k}\Omega$ resides in the region from $100\text{--}200\ \mu\text{m}$ from the tip, an additional $27\ \text{k}\Omega$ resides in the region from $200\text{--}300\ \mu\text{m}$; and about $37\ \text{k}\Omega$ occurs in the region from $300\ \mu\text{m}$ to $1\ \text{mm}$ from the tip. The region from $1\text{--}4\ \text{mm}$ from the tip adds another $12\ \text{k}\Omega$. It has been assumed that the capacitance is uniformly distributed along the pipette with a value of $1\ \text{pF/mm}$ of immersion. An Ag/AgCl wire extends into the pipette coming to within $4\ \text{mm}$ of the tip and it is assumed that the resistance of the pipette is negligible beyond the tip of the wire (due to the shunting effect of the wire). A noise equivalent circuit of the pipette can be created by lumping the resistance and capacitance of each small segment (*e.g.*, $20\text{--}50\ \mu\text{m}$) of pipette. The approximate circuit is then a ladder network formed of a series of resistors and their equivalent thermal voltage noise sources with a capacitor to ground at each node representing a portion of the pipette immersed in the bath. Rough calculations with such an equivalent circuit indicate that for a depth of immersion of $2\ \text{mm}$ the noise arising from this mechanism will be about $0.13\ \text{pA rms}$ in a $10\ \text{kHz}$ bandwidth. For a $1\ \text{mm}$ depth of immersion this value would fall to about $0.10\ \text{pA rms}$. For an idealized pipette identical to the one described here but with a cone angle of 22.6° (total resistance is about $1.6\ \text{M}\Omega$) these values fall to about $0.07\ \text{pA rms}$ for a $2\ \text{mm}$ depth of immersion and about $0.05\ \text{pA rms}$ for a $1\ \text{mm}$ depth of immersion, both for a $10\ \text{kHz}$ bandwidth. Over the frequency range of interest to patch voltage clamping, the PSD (Amp^2/Hz) of this noise should rise with increasing frequency as f^2 .

These calculated values are highly approximate and the assumed geometry is obviously an over-simplification. A variety of factors could increase the noise arising from this mechanism. For example, the noise should increase if there is an extended region behind the tip where the angle of taper is quite shallow, resulting in increased resistance in this region. Noise will also increase if the wire does not protrude as close to the tip as assumed above. In addition, some glasses tend to thin near the pipette tip, resulting in increased capacitance in this region. It should also be noted that shallow depths of immersion would not decrease this noise quite as much as might be expected since this would decrease the pipette capacitance, but not its resistance.

The noise from this mechanism can be reduced in several ways. From the above estimates it seems that noise arising from the distributed resistance and capacitance of the pipette should be smaller than the dielectric noise of pipettes fabricated from even the best known glasses. Nevertheless, with better (lower loss) glasses, particularly quartz, this mechanism could be the dominant source of noise from the pipette itself, and its reduction may become important. First, it is obvious that the geometry of the first few millimeters of the pipette



will be an important determinant of the magnitude of this noise; therefore, when possible, pipettes should be pulled to minimize the resistance distal to the tip. Anything that reduces the pipette capacitance per unit length will also reduce this noise. Thus, thick-walled pipettes and glasses with low dielectric constants should provide the best results in terms of noise. Perhaps of more practical importance, coating the pipette with Sylgard #184 can significantly reduce the pipette capacitance, and consequently reduce noise of the type considered here. However, as already noted, it is more difficult to build up a thick coat of Sylgard in the region within the first few hundred micrometers from the tip than in more distant regions. As was the case with dielectric noise, shallow depths of immersion will also reduce the noise arising from pipette resistance and capacitance. Finally, it should also be possible to reduce this noise regardless of the immersion depth by using a fine wire (Ag/AgCl or platinized Ag/AgCl possibly sharpened at the tip) that protrudes as far as possible toward the tip of the pipette. Such a wire will, in effect, short out (in a frequency-dependent fashion) the resistance of the pipette-filling solution in the region into which it extends; thus, while the pipette capacitance will be unaltered for any given depth of immersion, its resistance up to the end of the wire would be significantly reduced.

In 1992, Rae and Levis have introduced a technique that has been shown to minimize pipette noise arising from all of the mechanisms discussed above. In this technique, the surface of the bathing solution was covered with a layer of Silicone oil (#200 Fluid from Dow Corning, Midland, MI). With excised patches it was then possible to raise the tip of the electrode to within a few micrometers of the saline-oil interface; a sharp line of demarcation could be observed along the pipette at this interface. The electrical characteristics of this oil are apparently quite good², so that only the tip of the pipette that remains in saline appears to contribute to total noise. If 10 μm of the pipette tip remain in saline, it would be expected that the capacitance associated with this length should be roughly 0.01 pF. Dielectric noise associated with the immersed portion of the pipette should be about one tenth of the values predicted for a 1 mm depth of immersion. It should be reasonable to approximate distributed R-C noise in this situation by a lumped resistance equal to the resistance of the pipette other than that arising from the tip itself in series with approximately 0.01 pF. If this resistance is taken to be 2.5 M Ω , the expected noise is only about 7 fA rms in a 10 kHz bandwidth; even for 10 M Ω it is less than 15 fA rms in this bandwidth. The noise increment associated with the pipette capacitance and the headstage input voltage noise is also minimized in this arrangement since the capacitance remains essentially the same as that with the electrode in air. It should also be noted that even when patches cannot be excised, this approach can still be effective if the bath is designed so that the solution level can be lowered, thereby bringing the layer of silicone fluid very close to the cell surface.

² Although the dielectric characteristics of the specific Silicone fluid used in these experiments is not available, Table 2.5 of **Electronics Designers' Handbook** (1977, L. Giacoletto ed., McGraw-Hill) lists a dissipation factor (D) of 8.5×10^{-5} at 1 kHz and 2×10^{-5} at 100 kHz for Silicone fluid (methyl- or ethyl-siloxane polymer); the dielectric constant (ϵ) is 2.68.



Using quartz pipettes with this technique has resulted in noise levels in actual recording situations as low as 0.08 pA rms in a 5 kHz bandwidth (4-pole Butterworth filter). For these experiments, the Axopatch 200A was used with an open-circuit headstage noise of 0.057 pA rms in a 5 kHz bandwidth; with the holder and electrode attached, but with the electrode tip in air, noise typically increased to about 0.07 pA rms in this bandwidth. In several experiments it was shown that the total noise closely approximated the rms sum of the noise of the headstage plus holder/electrode (electrode in air) and the thermal current noise of the measured DC seal resistance. This implies that dielectric noise and "distributed R-C noise" of the pipette contributed only a negligible amount to total noise in this situation. Recently, Rae and Levis (1993) showed that quartz pipettes can be fabricated with the Sutter Instrument P-200 laser-based puller to yield lower noise than they previously achieved, obviating the need for Silicone oil.

Preliminary tests have also been made using this technique with pipettes fabricated from two other types of glass (Corning 7760, Kimble KG-12). Although the noise reduction was significant, results were never as good as those achieved with quartz. For example, the best results achieved with KG-12 were slightly more than 0.10 pA rms in a 5 kHz bandwidth, even when seal resistances in the range of 50 - 100 G Ω were obtained. For a total noise of 0.105 pA rms, and assuming that the headstage plus holder/electrode in air produced 0.075 pA rms and that a 50 G Ω seal produces 0.04 pA rms, all in a 5 kHz bandwidth, the pipette would be estimated to contribute about 0.06 pA rms in this bandwidth. On the basis of the above discussion, this is several times the amount of noise expected for a pipette fabricated from this glass with 10 μ m of its tip in saline. One possible explanation of at least part of this discrepancy would be to assume that the glass had thinned excessively near the tip. It is also possible that the noise attributed to the seal in arriving at this estimate is too low. More work will be needed to clarify this issue.

Noise Properties of Quartz Patch Pipettes

In Winter 1991-92 it became possible to routinely fabricate patch pipettes from quartz using the Model P-2000 puller from Sutter Instrument Company (Novato, CA). This puller uses a laser to overcome the extremely high melting temperatures needed to draw pipettes from quartz tubing. Preliminary results using Amersil T-08 quartz pipettes are quite encouraging. For the preliminary results reported here, it was difficult to pull small-tipped blunt pipettes with 1.65 mm OD 1.15 mm ID tubing. Pipettes fabricated from this tubing typically had a rather long and relatively narrow shank. This geometry is not ideal for the lowest possible noise. Even so, these pipettes produced significantly less noise than pipettes fabricated from the best glasses used previously (*e.g.*, 7760, 8161). In actual recording situations with pipettes immersed about 3 mm into the bath and with seal resistances \geq 50 G Ω , rms noise in a 5 kHz bandwidth was typically about 0.12 - 0.13 pA rms using an Axopatch 200A. Estimates of the contribution of the pipette to this noise were in the range of 0.075-0.09 pA rms in this bandwidth. With the new technique described above (Rae & Levis, 1992), which allows the pipette tip to be positioned within a few micrometers of a layer of Silicone oil covering the surface of the bath, background noise levels as low as 0.08 pA rms in a 5 kHz bandwidth have been achieved in actual single-channel recording situations with quartz pipettes. In such cases the contribution of the dielectric noise and distributed R-C noise of the pipette appears to be negligible in comparison to other noise sources.



More accurate estimates of the noise attributable to the pipette could be made by sealing quartz pipettes to Sylgard. A typical result for approximately a 3 mm depth of immersion is 0.115 pA rms in a 5 kHz bandwidth for pipettes coated with a thin layer of Sylgard to within about 100-200 μm of the tip. The power spectral density (PSD) of this noise was also measured. An estimate of the PSD attributable to the dielectric noise and distributed R-C noise of the pipette was obtained by subtracting from the total PSD the PSD of the headstage with the electrode in air with a correction made for the effects of the additional capacitance of the immersed pipette (about 2.6 pF) in conjunction with the headstage input voltage noise. The thermal current noise level associated with the DC seal was also subtracted. The resulting PSD was taken to be the best estimate of the noise attributable to the pipette per se. This PSD (Amp^2/Hz) increased with frequency with a slope of approximately $f^{1.85}$ in the frequency range from 2-20 kHz. From the PSD it could be estimated that the pipette accounted for about 0.07 pA rms of noise in a 5 kHz bandwidth and about 0.17 pA rms in a 10 kHz bandwidth. If it is assumed that the slope of $f^{1.85}$ was composed of a component with a slope of f attributable to the dielectric noise of the pipette and a component with a slope of f^2 , attributed to distributed resistance-capacitance noise of the pipette, it can be estimated that dielectric noise would account for slightly less than 0.06 pA rms in a 10 kHz bandwidth. Distributed R-C noise would then account for about 0.16 pA rms at this bandwidth. The estimated value of dielectric noise is somewhat higher than would be expected from the value of D listed for Amersil TO-8 quartz (0.0001 at 1 MHz) and the measured value of C_D (2.6 pF); with these values, equation 10 predicts ≈ 0.04 pA rms of dielectric noise in a 10 kHz bandwidth. If the above parsing of the noise components is correct, then it can be estimated that the actual value of D for the quartz used was closer to 0.00025. Even if this value is correct, the $D\epsilon$ product for this quartz is still about an order of magnitude lower than that of any other glass used to date for the fabrication of patch pipettes. At the time of this writing, neither different grades (*i.e.*, higher purity) of quartz from the same supplier nor quartz from other manufacturers have been investigated. It should also be noted that the noise component attributed to distributed R-C noise probably could have been reduced if the pipettes tested had a more favorable geometry.

When the same procedure was used to estimate the pipette noise when the depth of immersion was decreased such that the increment in capacitance was about 0.7 pF above that measured with the pipette tip just above the solution, it was found that the noise attributable to the pipette was roughly a factor of two lower than the figures reported above. In this case the estimated pipette noise PSD increased with increasing frequency approximately as $f^{1.9}$ in the range from 2-20 kHz. This is consistent with the prediction that the relative decrease in dielectric noise will be somewhat greater than that of distributed R-C noise as the depth of immersion decreases.

It should be noted that the results for quartz pipettes are qualitatively as well as quantitatively different from those that have been obtained previously from pipettes fabricated with other types of glass. Estimates of pipette noise based on procedures like those described above have been performed for many types of glass (*i.e.*, Figure 12-4). Even for the lowest $D\epsilon$ product glasses (*e.g.*, 7760, 8161, 7740), the estimated pipette noise PSD rises with increasing frequency as $f^{1.1}$ - $f^{1.3}$ (frequency range 2 - 20 kHz, immersion depth ≈ 2 mm). This indicates that dielectric noise dominates total pipette noise for these glasses. However, for quartz not only is the pipette noise significantly less for a given depth



of immersion, but the estimated pipette noise PSD rises much more steeply with increasing frequency ($f^{1.8}$ - $f^{1.9}$ in the 2-20 kHz frequency range)³. This indicates that dielectric noise is no longer the dominant source of noise for patch pipettes fabricated from quartz. The data described above are consistent with the interpretation that for quartz pipettes "distributed R-C noise" has become the dominant noise mechanism due to the greatly reduced contribution of dielectric noise. As more data from quartz pipettes becomes available these estimates and conclusions will doubtlessly be refined.

Noise Arising From Pipette Resistance and Patch Capacitance

The capacitance, C_p , of the patch is in series with the entire pipette resistance, R_e . The thermal voltage noise of R_e will produce current noise in conjunction with the patch capacitance. The PSD of this noise, $S_p^2(f)$, is given by:

$$S_p^2(f) = 4\pi^2 e_e^2 C_p^2 f^2 \quad (14)$$

where $e_e^2 = 4kTR_e$ is the thermal voltage noise of the pipette. The rms noise arising from this mechanism from DC to a bandwidth B is then $(\frac{4}{3}\pi^2 e_e^2 C_p^2 B^3)^{1/2}$. In general, this noise should be quite small, but it can become significant when the patch area is large; *e.g.*, when a large "bleb" of membrane is sucked into the pipette tip. Sakmann and Neher (1983, in **Single-Channel Recording**, Sakmann, B. and Neher E. eds. pp. 37-51) measured patch capacitance for a large number of pipettes with resistances ranging from about 1 - 10 M Ω . They found that the value of C_p varied from as little as 0.01 pF to as much as 0.25 pF. Despite a very large amount of scatter, they found that C_p and R_e were correlated, with C_p increasing as R_e decreases. The best fit to their data was $C_p = 0.126 \text{ pF} / (R + 0.018)$, where R is the pipette resistance in M Ω . Using this average relationship it can be predicted that for a "typical" 10 M Ω pipette ($C_p = 0.015 \text{ pF}$) the noise in a 10 kHz bandwidth (8-pole Bessel filter) arising from this mechanism will be about 0.03 pA rms, while for a 1 M Ω pipette (typical $C_p = 0.128 \text{ pF}$) this value will increase to 0.08 pA rms. Sakmann and Neher's results indicate that in the most favorable situations in terms of " R_e - C_p " noise, the rms noise from this mechanism can be as low as 0.01 pA rms in a 10 kHz bandwidth. However, in the least favorable situation ($R_e \approx 2 \text{ M}\Omega$, $C_p \approx 0.25 \text{ pF}$) the noise from this mechanism can be as large as 0.23 pA rms in a 10 kHz bandwidth (8-pole Bessel filter).

Seal Noise

The membrane-to-glass seal that is essential to the patch voltage-clamp technique is the final source of noise associated with the pipette that will be considered here. Seal noise is perhaps the

³ Note, however, that the PSD for quartz pipettes is lower than that of pipettes made from other glasses at all frequencies measured. At sufficiently high frequencies distributed R-C noise should dominate the total noise for pipettes fabricated from *any* type of glass. However, for quartz pipettes the PSD of distributed R-C noise should exceed that of dielectric noise by 1 kHz; for pipettes made from 7760, distributed R-C noise should not exceed dielectric noise up to 10-20 kHz, and for soda lime (*e.g.*, 0080) pipettes this frequency might be closer to 100 kHz or more. Distributed R-C noise depends on the pipette geometry and a variety of other factors already described; the only influence of the glass type itself — accept in so far as it effects the geometry which can be pulled — is its dielectric constant.



least understood source of noise in the patch clamp technique. The power spectral, $S_{sh}^2(f)$, of the noise arising from the seal for zero applied voltage is given by:

$$S_{sh}^2(f) = 4kT \operatorname{Re}\{Y_{sh}\} \quad (15)$$

where $\operatorname{Re}\{Y_{sh}\}$ is the real part of the seal admittance Y_{sh} . The minimum estimate of seal noise results from the assumption that $\operatorname{Re}\{Y_{sh}\} = 1/R_{sh}$, where R_{sh} is the DC seal resistance. If this assumption is correct, then for a 10 kHz bandwidth, seal resistances of 1, 10 and 100 G Ω would produce noise of 0.4, 0.13 and 0.04 pA rms, respectively. Since values of R_{sh} in the range of 100-200 G Ω are not uncommon, this would imply that the noise associated with a very tight seal would be small in comparison with other sources of patch-clamp noise. However, it is possible that the PSD of seal noise may rise above the minimum level given by $4kT/R_{sh}$ as frequency increases (*i.e.*, the real part of the seal admittance may increase with frequency) due to the capacitance of the glass and the membrane which make up the wall of the seal. Unfortunately, we have no good theoretical basis upon which to estimate Y_{sh} since the precise nature of the membrane-glass seal is not known.

It is also very difficult to empirically dissect out the noise associated with the seal from total patch clamp noise. We believe that previous attempts to do this have overestimated this noise. For example, as shown in Figure 1-11 of Sigworth (1983), data from F. Sachs and E. Neher indicate a frequency-dependent seal noise PSD ($R_{sh} \approx 20$ G Ω) that would amount to at least 0.13 pA rms in a bandwidth from DC to 5 kHz. However, with an integrating headstage (*e.g.*, the CV 201A or 202A of the Axopatch 200A), total noise levels (*i.e.*, including the noise of the headstage, holder, pipette, seal, etc.) lower than this value have often been achieved in the same 5 kHz bandwidth in actual recording situations.

Rae and Levis have reported in 1992 measurements using an Axopatch 200A with quartz pipettes and a novel technique involving placing a layer of Silicone oil on the surface of the bathing solution containing the cells to be patched. This technique allows excised patches to be brought within a few micrometers of the oil-water interface, thereby minimizing the noise contribution of the pipette. With this approach, total noise levels as low as ≈ 0.08 pA rms in a 5 kHz bandwidth were achieved. In several experiments with excised patches, the DC seal resistance was measured (range 40 - 60 G Ω) and the noise was measured with the tip just beneath the layer of oil and again with the tip withdrawn into the oil. The rms difference of these two noise measurements should be dominated by the seal noise plus the small amount of noise arising from the pipette resistance in series with the patch capacitance. In all cases, it was found that this rms difference for a bandwidth of 5 kHz was close to the thermal current noise predicted from a measured seal resistance (*i.e.*, $(4kTB/R_{sh})^{1/2}$). Nevertheless, it is well known to anyone who has struggled to achieve the lowest possible noise in patch-clamp measurements that there is considerable variability in the total noise even among patches with very high seal resistances and with all other conditions seemingly identical. Despite the conclusions drawn above, it seems reasonable to guess that some of this variability arises from the seal. Noise associated with the membrane-glass seal represents one of the fundamental limitations of the patch clamp technique, but it now seems clear that under favorable conditions such noise can be as low as 0.03 pA rms in a 5 kHz bandwidth. Recently, Rae and Levis (1993) achieved ultra low-noise recording without silicone oil by improving the fabrication of the quartz pipettes.



Noise in Whole-Cell Voltage Clamping

The noise associated with the whole-cell variant of the patch voltage-clamp technique at moderate to high frequencies will almost always be dominated by current noise arising from the series (pipette) resistance R_s , in conjunction with the membrane capacitance, C_m , of the cell. It should be noted that the measured value of R_s is often 2 or even 3 times higher than the resistance of the pipette prior to achieving a whole-cell recording. Due to the filtering effect of the access resistance and cell capacitance, series-resistance compensation is required to increase the actual bandwidth of current measurement beyond $1/2\pi R_s C_m$. The level of series-resistance compensation is an important determinant of whole-cell voltage clamp noise as well as of the bandwidth and fidelity of recording (see more on series-resistance compensation in **Chapter 3**). The voltage noise PSD of R_s is approximated by $4kTR_s$ (V^2/Hz). It should be noted, however, that in addition to thermal noise a $1/f$ component is expected, particularly when relatively large currents are passed through the pipette. The PSD, $S_{wc}^2(f)$, of the current noise arising from R_s and C_m is given by:

$$S_{wc}^2(f) = \frac{4\pi^2 f^2 e_s^2 C_m^2}{1 + 4\pi^2 f^2 \tau_{sr}^2} \quad (\text{units: Amp}^2/\text{Hz}) \quad (16)$$

where $e_s^2 = 4kTR_s$ and $\tau_{sr} = R_{sr}C_m$ and R_{sr} is the residual (*i.e.*, uncompensated) series resistance, *e.g.*, if $R_s = 10$ M Ω then for series-resistance compensation levels of 50%, 70% and 90%, R_{sr} will be 5 M Ω , 3 M Ω and 1 M Ω , respectively. It should be noted that for 100% series-resistance compensation, equation (16) reduces to $4\pi^2 f^2 e_s^2 C_m^2$. This emphasizes that series-resistance compensation (if it is properly designed) only restores the noise to the level that would have resulted from the thermal voltage noise of R_s in series with C_m in the absence of the filtering effect of R_s mentioned above. The rms noise arising from R_s and C_m over a bandwidth from DC to B Hz can be obtained by integrating equation (16) over f from 0 to B.

Patch clamps commonly use (switch in) a 500 M Ω feedback resistor for whole-cell voltage clamping. The noise of this resistor dominates open-circuit headstage noise up to bandwidths of about 10 kHz. However, for typical cells the noise arising from R_s and C_m will be larger than that of the headstage for all bandwidths above a few hundred Hz. Even for relatively ideal situations in terms of noise (*e.g.*, a small cell with $C_m = 5$ pF voltage clamped through $R_s = 5$ M Ω), the noise of a 500 M Ω feedback resistor will not dominate total noise for bandwidths above about 1 kHz. Figure 12-4 shows the noise PSD and rms noise for a typical whole-cell voltage clamp situation with $R_s = 10$ M Ω and $C_m = 33$ pF (these are the values used in the Model Cell provided with the Axopatch-1 and the Axopatch 200 series of patch clamps). The top panel shows the noise PSD (as computed from equation 16 plus headstage noise) for series-resistance compensation levels of 0%, 50%, 70% and 90%; the noise PSD of an open-circuit headstage alone is shown for comparison. It is instructive to derive an expression for the high frequency plateau of these PSDs (from equation 16). If the fraction of series-resistance compensation is defined as α and $\beta = 1 - \alpha$ (*e.g.*, for 80% compensation $\beta = 0.2$; also note that $R_{sr} = \beta R_s$), then as $f \rightarrow \infty$, $S_{wc}^2(f) \rightarrow 4kT/(\beta^2 R)$. Even without series-resistance compensation ($\beta = 1$) the high frequency plateau is $4kT/R_s$; *i.e.*, 50 times larger than that of a 500 M Ω resistor. With 90% compensation ($\beta = 0.1$) the plateau level is $4kT/(0.01R_s)$, which, in this case, is equivalent to the thermal current noise of a 100 k Ω resistor.



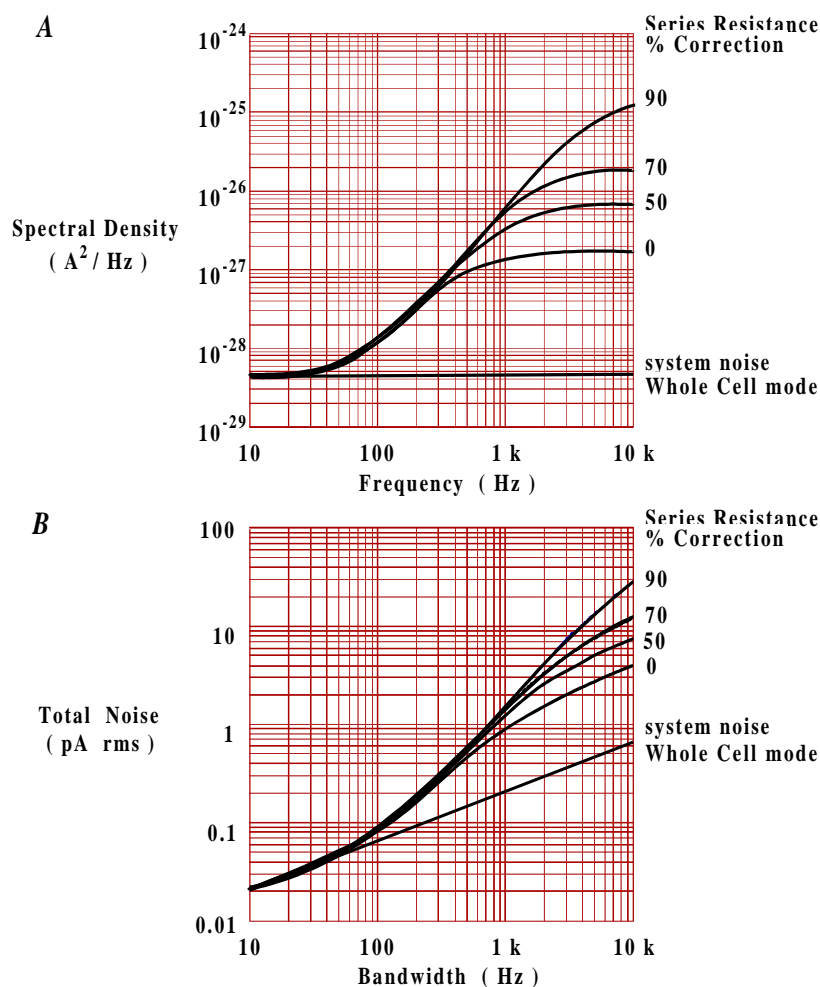


Figure 12-4. Noise in Whole-Cell Voltage Clamping

A. Power spectral density as a function of frequency for a whole-cell voltage clamp.

Cell membrane capacitance is 33 pF and series resistance is 10 M Ω ; cell input resistance has been assumed to be much larger than 500 M Ω . Series resistance compensation levels of 0%, 50% and 90% are shown. The lower curve (system noise) approximates the open circuit headstage noise in whole-cell mode with a feedback resistor of 500 M Ω .

B. rms noise as a function of bandwidth for the same whole-cell voltage clamp situation illustrated in A.

Note that the headstage noise dominates total noise in this situation only at bandwidths less than \approx 100 Hz.

The lower panel of Figure 12-4 shows the total rms noise as a function of bandwidth for the same cell parameters with R_s compensation levels of 0%, 50%, 70% and 90%; the rms noise of the open circuit headstage is also shown. Note that by a bandwidth of only about 200 Hz the total noise is twice that of the headstage alone; therefore, even if a headstage with negligible noise had been used, at this bandwidth total noise would only decline to about 70% of the value shown. As



the bandwidth of current measurement increases, the noise of the headstage itself becomes progressively more negligible; with 90% compensation at a bandwidth of 1 kHz, a headstage with no noise would have reduced total noise by less than 1% (recall that the noise of the headstage and the R_s - C_m noise considered here are not correlated and, therefore, add in an rms fashion). It should also be pointed out that the bandwidths in this figure refer to the setting of an external filter (a perfect "brick-wall" filter has been assumed, see below). But it is important to realize that the actual bandwidth of current measurement is limited to $1/2\pi R_{st} C_m$ (1 pole RC filter). Without series-resistance compensation, in this example the bandwidth is only about 480 Hz and the use of external filter bandwidths much above this will only add noise, not new signal information. The effective bandwidth increases with increasing series-resistance compensation, reaching nearly 5 kHz with 90% compensation.

External Noise Sources

Interference from external sources can be almost completely eliminated in a well-designed system, but can become the dominant source of noise if proper precautions are not taken. The most familiar form of interference is line-frequency pickup (50 or 60 Hz and harmonics) from power supplies, fluorescent lights, etc. Well-designed instruments will not introduce significant amounts of interference from their internal power supplies. However, a typical laboratory environment is full of potential sources of interference from sources external to the electronic instrumentation involved in a particular measurement. In addition to line-frequency pickup, other potential sources of interference include nearby motors, elevators, radio and television stations, and the video monitor of your computer (which produces an annoying timing signal at 16 kHz or higher frequency). High impedance measurements, such as patch clamping or work with intracellular microelectrodes, are particularly sensitive to such external interference.

In most cases such noise sources can be controlled by careful grounding, shielding and filtering. (For a detailed discussion of these techniques see **Chapter 2**). In some situations, however, shielding can actually increase noise. An example is metal shielding of the pipette holder used in the patch clamp. Such shielding inevitably increases the capacitance at the input of the amplifier (C_g in equations (11) - (13) above) by several picofarads. Even if the *mean voltage* on the shield is precisely the same as that of the negative input of the amplifier, the *noise voltages* will differ and lead to increased high frequency noise. For this reason Axon Instruments does not offer or recommend such shielded holders; it is our experience that grounding of nearby metal objects, such as the microscope, usually provides adequate shielding. Vibration, either transmitted through the floor or through the air, is another source of external interference and adequate vibration isolation is almost always required for sensitive electrophysiological measurements.

Digitization Noise

Noise arising from digitization is often ignored. Sometimes this is justified since such noise can be negligible with respect to other sources of noise. However, in some situations this potential source of noise can become significant. In order to ensure that this noise remains negligible one needs to understand the types of noise that can arise from digitization and to use analog to digital converters, preamplifiers, filters, etc. that are appropriate for the measurement of the signal.



Quantization is the approximation of each value of a signal by an integer multiple of an elementary quantity δ , which is the quantizing step. For a 12-bit analog-to-digital converter (ADC) with full-scale range (FSR) of ± 10 V, $\delta = 20\text{V}/2^{12} = 4.88$ mV; for a 16-bit converter with the same FSR, $\delta = 305$ μV . This approximation leads to the addition of a noise signal, called *quantizing noise*, to the original signal. When the signal being digitized is reasonably large relative to the quantizing step δ , the power of the quantizing noise can usually be approximated by:

$$\frac{\delta^2}{12}$$

and the rms value of the quantizing noise is therefore:

$$\sqrt{\frac{\delta^2}{12}}$$

For a 12-bit ADC with a 20 V FSR this noise value is 1.41 mV rms or about 8.5 mV peak-to-peak.

In the process of analog-to-digital conversion, the signal is sampled as well as quantized. The sampling frequency is denoted by f_s ; *e.g.*, when converting at 1 point every 10 μs , f_s is 100 kHz. In this case all of the quantizing noise power in the ADC output will appear in the frequency band from DC to $f_s/2$. The PSD is usually white (*i.e.*, constant over the frequency band) and has a value of $\delta^2/6f_s$.

It is obvious that the quantizing step δ should be small relative to the signal being measured. This is easily accomplished in most situations by the use of appropriate preamplification to scale the desired signal such that it fills a reasonable portion of the dynamic range of the ADC. Difficulties can arise, however, if you need to measure small changes embedded in large signals. Analog instruments can often have a dynamic range that considerably exceeds that of ADCs. Again, using the capacitive-feedback patch clamp as an example, noise levels as low as 0.02 pA rms can be achieved at a bandwidth of 1 kHz; moreover, such an instrument can achieve noise this low even with a gain as low as 100 $\mu\text{V}/\text{pA}$. This would amount to an rms noise of only 2 μV . In order to utilize the full dynamic range of such an instrument at this bandwidth, an ADC with 22-bit resolution (and capable of sampling at 2 - 5 kHz) would be required. To the best of our knowledge, this much dynamic range is not required for electrophysiological measurements and 12- to 16-bit resolution in conjunction with a variable amount of preamplification is quite adequate (see **Chapter 9** for further discussion).

Aliasing

A signal can be determined completely by a set of regularly spaced samples at intervals $T = 1/f_s$ only if it does not contain components with a frequency equal to or greater than $f_s/2$. This is basically a statement of the sampling theorem; f_s is just the sampling frequency mentioned above. The term $f_s/2$ will be denoted by f_n and is often called the *Nyquist frequency* or *folding frequency* for reasons that will be described below. Another way of putting this is that for



sampled data, frequency is only defined over the range from 0 to f_n ; components with frequencies higher than f_n cannot be described (at least 2 points per cycle are needed to uniquely define a sine wave). Obviously there is nothing (other than good sense) that will stop one from digitizing a signal with frequency components extending many times beyond f_n . However, digitizing frequency components of the signal that lie above f_n will result in "folding back" of these higher frequency components into the frequency range from 0 to f_n , consequently producing aliases.

The term f_n is referred to as the folding frequency because the frequency axis of the power spectral density will fold around f_n in a manner similar to folding a road map or a carpenter's scale. This folding effect is illustrated in Figure 12-5; frequency components above f_n are shifted to lower frequencies (in the range 0 to f_n). If f_x is the frequency of a signal component (desired or noise) above f_n , then the frequency of its alias, f_a , is given by:

$$f_a = |f_x - kf_s| \quad (17)$$

where the brackets, $| \quad |$, indicate absolute value, f_s is the sampling frequency, and k is a positive integer taking on whatever value is required so that f_a falls in the range $0 \leq f_a \leq f_n$. For example, with $f_s = 20$ kHz ($f_n = 10$ kHz), a frequency component at 18 kHz will alias to a component at 2 kHz ($f_a = |18 \text{ kHz} - 1 \times 20 \text{ kHz}| = 2 \text{ kHz}$) in the digitized waveform. Similarly, as shown in Figure 12-5, frequency components at 22 kHz, 38 kHz, 58 kHz, 62 kHz, etc. will all alias to 2 kHz in the sampled data.

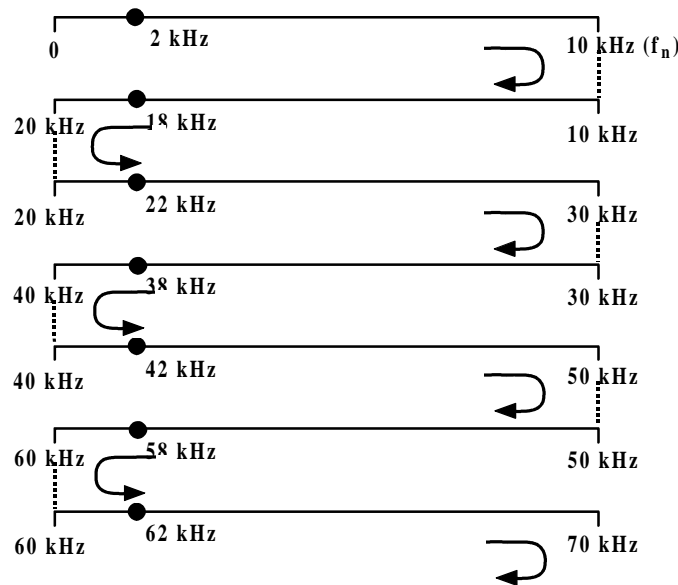


Figure 12-5. Folding of the Frequency Axis

In this folding of the frequency axis for $f_s = 20$ kHz ($f_n = 10$ kHz), note that all of the round points shown (18 kHz, 22 kHz, ...) alias to 2 kHz.

As an example of aliasing and the problems it can produce, consider white noise extending from DC to 10 MHz. To be specific we will assume that the PSD of this noise is 10^{-14} V²/Hz (100 nV/ $\sqrt{\text{Hz}}$); the total noise in the 10 MHz bandwidth is then 316 μV rms (about 2 mV peak-to-peak). If this noise is sampled at $f_s = 20$ kHz without the use of an anti-aliasing filter, it should



be obvious that the rms value of the sampled points will be the same as that of the original data, *i.e.*, 316 μV . However, the sampled data cannot describe any frequency component greater than f_n , here 10 kHz. If a smooth curve is fitted through the sampled points (*e.g.*, using a cubic spline), you will find that the noise appears to be bandlimited from DC to 10 kHz and that its amplitude is the same as the original data; its power spectral density will be $10^{-11} \text{ V}^2/\text{Hz}$, *i.e.*, 1,000 times higher than that of the original data because the sampling has folded over the original spectrum 1,000 times. The frequency components above 10 kHz have all been aliased into the frequency band extending from DC to f_n . Clearly, aliasing has not increased the total amount of noise, but it has shifted it from higher to lower frequencies. It is worth considering what will happen if the sampled data is subsequently digitally filtered with a cutoff frequency of 1 kHz. This will result in reducing the noise from 316 μV rms to 100 μV rms. However, if the original noise signal had been passed through an analog filter with the same cutoff frequency (1 kHz), the noise amplitude would have been reduced to only 3.16 μV rms. Once aliasing has occurred it cannot be undone by any digital operation. The solution here is either to sample much faster ($> 20 \text{ MHz}$ in this example) or, if a 20 kHz sample rate is required, to use an analog anti-aliasing filter to adequately reduce the amplitude of all frequency components above 10 kHz.

If the PSD of the noise is not white but instead rises as f^2 with increasing frequency — as is the case for high frequency noise from a patch voltage clamp — the consequences of aliasing can be even more severe. As an extreme example, consider a voltage noise of $100 \text{ nV}/\sqrt{\text{Hz}}$ in series with a 10 pF capacitor (see equation (13) and related discussion); in a 10 MHz bandwidth this would produce a current noise of 115 nA rms. Again, assuming a digitization rate of 20 kHz with no anti-aliasing filter, all of this noise would be aliased into the frequency band from DC to 10 kHz, even though the noise in a bandwidth of 10 kHz would have only been about 3.6 pA rms. Moreover, subsequent digital filtering of the digitized noise with a cut-off frequency of 1 kHz, as in the previous example, would only reduce the noise amplitude to about 35 nA rms, whereas an analog filter set to a 1 kHz bandwidth would have reduced the noise to only 0.115 pA rms — 300,000 times less than achieved by digitally filtering the aliased noise. Of course patch clamps do not have a bandwidth of 10 MHz; even with more realistic bandwidths, failure to use proper anti-aliasing filters can greatly increase noise beyond that existing in the bandwidth resolved by the digitization process (*i.e.*, f_n) and can reduce the effectiveness of subsequent digital filtering of the data.

It should be noted that in the above examples it has been assumed that the filter used had an abrupt cut-off at its -3 dB bandwidth. This will normally not be the case when measuring signals in the time domain. Filters with Gaussian or Bessel characteristics (as are used most frequently for electrophysiological measurements) roll off quite gradually beyond their -3 dB bandwidth (f_c) and it is therefore not appropriate when using such filters to eliminate aliasing to set $f_c = f_n$. Recall that the requirement to avoid significant aliasing is that all frequency components above f_n must be adequately attenuated. When using a Bessel filter (typically 4- or 8-pole) for anti-aliasing, the choice of the cut-off frequency relative to f_n depends on the characteristics of the noise and how much aliasing can be tolerated. We advise the use of $f_c \leq 0.4 - 0.5f_n$ ($0.2-0.25f_n$) as a useful and generally reasonable practice.



Filtering

The above discussion naturally leads to a brief discussion of filtering. In general, the bandwidth of a filter is selected to reduce noise to acceptable levels so that the desired signal can be adequately observed. As described above, filtering prior to digitization is also necessary to prevent aliasing. If the signal to be measured is large in comparison with the background noise, then the filter bandwidth — and the appropriate digitization rate — can be chosen on the basis of the desired time resolution; wider bandwidths allow more rapid events to be resolved. However, in many electrophysiological measurements very wide bandwidths will result in background noise levels that will obscure the signals of interest. In such situations it is necessary to make compromises between the amount of noise that can be tolerated *vs.* the time resolution that is achieved after filtering.

There is an interesting — although perhaps unfortunate — relationship between a function and its Fourier transform: as the function gets narrower its transform becomes wider. The impulse response of a filter (time domain; note that the integral of the impulse response is the step response) and its transfer function (frequency domain) are a Fourier transform pair. There are limits on the degree to which signals can be simultaneously "concentrated" in both the time and the frequency domain (in fact, if stated formally, this is the *uncertainty principle* in the units we are using). In practical terms this means that a filter with a narrow impulse response, and therefore a rapid risetime, will have a rather gradual roll-off in the frequency domain. Conversely, a filter with a sharp cut-off in the frequency domain will have a more spread-out impulse response and slower risetime.

Among commonly used filters, those that provide the best resolution with little or no overshoot and ringing of the step response are the Gaussian and Bessel filters (as the order of a Bessel filter increases it more closely approximates a Gaussian filter). A true Gaussian filter is easy to implement digitally, but is not often produced as an analog filter (although passive filters that are a good approximation of this type can be constructed). Bessel filters are more commonly used in analog applications. The basic characteristics of both filter types is quite similar. A Gaussian filter has an impulse response with the shape of the Gaussian distribution; its step response has no overshoot. The 10 - 90% risetime of the step response of a Gaussian filter is approximately $0.34/f_c$, where f_c is the -3 dB bandwidth in hertz. However, in the frequency domain the roll-off of this filter is quite gradual. Denoting the transfer function by $H(f)$, $H(f_c) = 0.707$ (-3 dB), $H(2f_c) = 0.25$ (-12 dB), and $H(3f_c) = 0.044$ (-27 dB). An 8th-order Bessel filter closely approximates this response in both the time domain and the frequency domain. Clearly, in terms of noise reduction, a filter whose transfer function rolls off much more quickly after it reaches f_c would appear to be desirable. Analog filters with such characteristics are readily available (*e.g.*, Elliptical and Chebyshev types); in fact, you can buy sharp cut-off filters with $H(f) = 0.01$ (-40 dB) when $f = 1.06f_c$. Digital filters can achieve even sharper cut-offs. Unfortunately, however, sharp cut-off filters are characterized by severe overshoot and prolonged ringing in their step responses. Additionally, for a given value of f_c , their risetimes can be nearly twice that of a Gaussian or Bessel filter. Because of this, very sharp cut-off filters are desirable for frequency domain measurements but quite undesirable for measurements in the time domain. In fact, in order to achieve the same time resolution with a sharp cut-off filter that is achieved with a Gaussian or Bessel filter it is necessary to use a higher value of f_c . In this case, the sharp cut-off filter (with its higher f_c) will pass as much or even more noise (depending on the spectral characteristics of the noise) as the more gradual roll-off Gaussian or Bessel filter when the two



have been set to provide essentially equivalent time resolution (as judged by step response risetime; see below). Some "exotic" filter types can produce the same risetime as the Gaussian filter with minimal overshoot and reduce the noise by a small amount; however, unless the noise PSD rises very steeply with increasing frequency, the improvement is only a few percent.

It is instructive to quantitatively compare the performance of a Gaussian or Bessel filter with a very sharp cut-off filter for time-domain measurements. When the underlying signal to be resolved is a square pulse, as is the case with single-channel currents, it is reasonable to relate the time resolutions of the filter to its 10-90% rise time. For single-channel measurements time resolution is often thought of in terms of the minimum detectable event duration. To some extent, of course, such a minimum duration is dependent on the detection algorithm used. Even so, it is reasonable to approximate the minimum detectable duration in terms of the filter bandwidth as $1/T_r^4$, where T_r is the 10-90% risetime of the filter. With such an operational definition of time resolution — or minimum detectable duration — it is possible to compare the performances of different filter types. As already noted, for a Gaussian or Bessel filter (8th order) $T_r \approx 0.34/f_c$, where f_c is the -3 dB bandwidth in hertz. A 10th-order Chebyshev filter (0.1 dB pass-band ripple) is a reasonable selection to approximate the "brick wall" characteristic mentioned above; for this filter $H(1.09f_c) = 0.1$ (-20 dB), $H(1.22f_c) = 0.01$ (-40 dB), and $H(2f_c) = -95$ dB. However, for this filter $T_r \approx 0.58/f_c$, *i.e.*, approximately 1.7 times the risetime of a Gaussian or Bessel filter with the same f_c . Moreover the step response is characterized by a peak overshoot of about 20% and sustained ringing which is noticeable up to about $10/f_c$. In order to achieve the same 10-90% risetime with the 10th-order Chebyshev filter that is achieved with a Gaussian or 8th-order Bessel filter, it is necessary to select the -3 dB bandwidth of the Chebyshev filter to be about 1.7 times higher than the -3 dB bandwidth of the Gaussian or Bessel filter. For example, the risetime of a Chebyshev filter with $f_c = 17$ kHz will be approximately the same as that of a Gaussian or Bessel filter with $f_c = 10$ kHz; it should be noted that the step response of the Chebyshev filter will ring severely. Even if the ringing of its step and impulse response is ignored so that it is assumed that the 10th-order Chebyshev filter and the Gaussian or Bessel filter have the same time resolution provided that f_c (Chebyshev) $\approx 1.7f_c$ (Gaussian), it is found that the Gaussian or Bessel filter significantly out-performs the Chebyshev filter in terms of noise in the filtered signal. For white noise it would be found that the Chebyshev filter would pass approximately 1.3x the noise passed by the Gaussian or Bessel filter, provided, of course, that both filters had the same 10-90% rise time. For noise with a PSD that rises as f^2 , the Chebyshev filter would actually pass about 1.5x the rms noise passed by the Gaussian or Bessel filter, again provided that the filters corner frequencies were set to produce the same risetime. Obviously, when time resolution is considered, extremely sharp cut-off filters are **not** the best selection. Sharp cut-off filters should only be used when frequency domain data (*e.g.*, power spectral density) is being collected.

Finally, as an illustration of the distinction between the -3 dB bandwidth and the uppermost frequency component of noise that can pass through a Gaussian or Bessel filter, consider a noise process ($e^2(f)$) whose PSD (V^2/Hz) rises as f^2 with increasing frequency. On linear scales such noise is shown in Figure 12-6 along with the transfer function of a Gaussian filter (squared,

⁴ For a 50% threshold-crossing detection algorithm as is commonly used with single-channel data and a Gaussian or Bessel filter, an event can be detected until its duration falls below about $0.54T_r$. It is certainly true that it is possible in principle to detect the occurrence of an isolated event of considerably shorter duration than T_r , but our objective here is to consider practical situations in which the event may not be isolated and must be characterized as well as simply detected.



$H^2(f)$) and the noise PSD that will be observed at the filter output (*i.e.*, $H^2(f)e^2(f)$). Note that the square root of the integral of the filtered noise PSD (*i.e.*, the square root of the area under the curve) will be the rms noise. The PSD of the filtered noise does not fall sharply at f_c . In fact, the filtered PSD reaches its peak at about $1.2 f_c$ and does not fall to negligible levels until more than $3 f_c$. This must be remembered when selecting a digitizing rate for any particular -3 dB filter setting if aliasing is to be avoided. In comparison with a filter with a "brick wall" roll-off at the same f_c , the Gaussian filter will have somewhat more than 40% more noise at its output. But recall that the sharp cut-off filter will have a much poorer time-domain response. In fact, as described above, if the -3 dB bandwidth of the sharp cut-off filter is selected to produce essentially the same time resolution as the Gaussian or Bessel filter, it will pass even more noise in this situation.

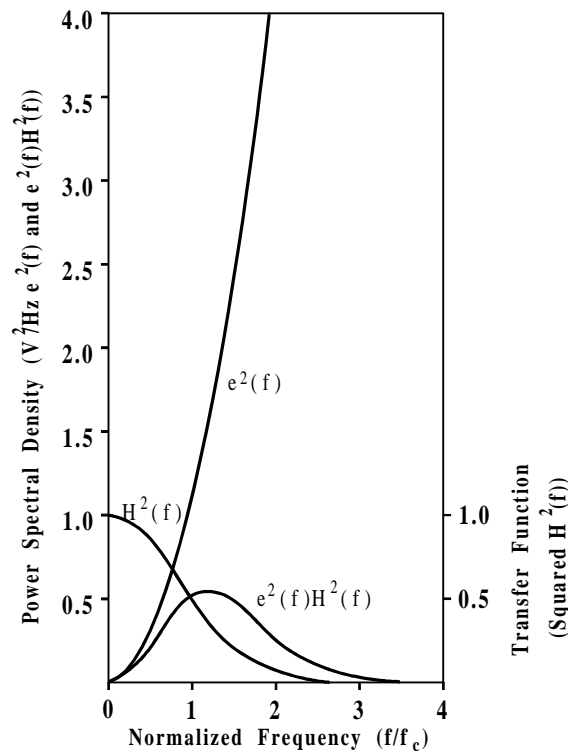


Figure 12-6. Squared Transfer Function of a Gaussian Filter

Illustrated are squared transfer function of a Gaussian filter ($H^2(f)$); noise process with PSD that arises as f^2 with increasing frequency ($e^2(f)$); and the same noise process PSD after passing through the Gaussian filter ($e^2(f)H^2(f)$). The scales are linear; frequency is normalized to the -3 dB bandwidth (f_c) of the filter; PSD scale is arbitrary. Note that due to the gradual roll-off of the Gaussian filter, the filtered noise still has significant power well beyond f_c .

A useful alternative to adjusting the analog filter bandwidth to attempt to achieve an optimum signal-to-noise ratio is to digitize the data at a rapid rate through a Bessel filter with its -3 dB bandwidth set to prevent aliasing. The wideband digitized data may then be filtered digitally to achieve an acceptable signal to noise level. The digital filter should once again generally be of the Gaussian or Bessel type. In such situations more than one filter are used in series; if these are all of the Gaussian or Bessel type, then the final -3 dB bandwidth, f_{cF} , is approximately given by:



$$f_{cF} = \frac{1}{\sqrt{\frac{1}{f_1^2} + \frac{1}{f_2^2} + \frac{1}{f_3^2} + \dots}}$$

where $f_1, f_2, f_3 \dots$ are the -3 dB bandwidths of the individual filters in series. Of course, the same expression holds for a series combination of analog filters. The disadvantage to this general approach is that initial data storage will be increased due to the high digitization rate; once the data has been digitally filtered it can also be decimated if desired.

Summary of Patch-Clamp Noise

Headstage

At the time of publishing this **Guide**, the best capacitive-feedback headstages (the CV 201A and CV 202A of the Axopatch 200A) have an open-circuit noise of about 0.13 pA rms in a 10 kHz bandwidth (-3 dB, 8-pole Bessel filter). Resistive-feedback headstages have noise of about 0.25-0.30 pA rms in this bandwidth. It is likely that developing capacitive-feedback technology over the next few years will further yield improvements in noise. In fact, in theory, it should be possible to produce a capacitive-feedback headstage with noise that is only about half of that achieved presently.

Holder

The pipette holder contributes noise by increasing the capacitance at the headstage input; some dielectric noise must also be expected. The unshielded polycarbonate holders provided by Axon Instruments by themselves will only increase the headstage noise by about 10% above its open circuit value even for the lowest noise capacitive-feedback devices. For example, for the Axopatch 200A with an open-circuit noise of 0.060 pA rms in a 5 kHz bandwidth (as shown on the panel meter), the total noise with the holder attached should not increase beyond 0.070 pA rms (note that larger noise increments probably mean that the holder needs to be cleaned), and will often be as low as 0.065 pA rms. Inserting a saline-filled electrode into the holder will further increase noise even while the electrode tip is in air. With a saline-filled electrode, the noise of the Axopatch 200A with an open-circuit noise of 0.060 pA in a 5 kHz bandwidth will generally increase to about 0.075 pA rms.

Electrode

The noise associated with the patch pipette is determined by the type of glass used, the wall thickness of the glass, the pipette geometry, the use of Sylgard coating, and the depth of immersion into the bath. At the present time, dielectric noise is probably the dominant source of noise associated with the electrode for all glasses except quartz. For glasses with lower $D\epsilon$ products — most notably quartz — it can be expected to become a much smaller component of overall noise. Additional noise will arise from the distributed resistance and capacitance of the pipette. For the best glasses presently in common use this source of noise is probably somewhat less than the dielectric noise of the glass; for very low-loss glasses, such as quartz, it could be the dominant source of pipette noise. A small amount of noise will also result from the thermal



noise of the pipette resistance in series with the patch capacitance; only under certain situations (a large patch area) will this " R_e - C_p " noise become significant.

Theoretical and experimental results indicate that a pipette fabricated from the lowest-noise glasses (other than quartz) used to date (Corning #7760, #8161) with a moderate coating of Sylgard will produce noise of about 0.2 pA rms in a 10 kHz bandwidth (8-pole Bessel filter) for an immersion depth of about 2 mm. Under favorable circumstances this value can be cut at least in half when the tip of the pipette is withdrawn to within 100-200 μm of the surface of the bath. For pipettes fabricated from quartz, preliminary results indicate that for a 1 mm depth of immersion, noise of somewhat less than 0.1 pA rms can be expected in a bandwidth of 10 kHz; with the very small immersion depth possible (10 μm or less) with the Silicone-fluid technique described above, it can be estimated that the noise contributed by a quartz pipette falls to less than half of this value. To date the only results obtained for quartz have involved pipettes with relatively long narrow shanks and resistances of roughly 10 M Ω . Such a geometry is not ideal for achieving the lowest possible noise. As techniques for pulling quartz pipettes improve, and as other grades and suppliers of quartz are investigated, further improvements are likely.

Seal

The noise associated with the seal is less easily predicted. Certainly a minimum estimate of this noise in a bandwidth B is given by $(4kTB/R_{sh})^{1/2}$, i.e., the thermal current noise of the DC seal resistance, R_{sh} . For excellent seals in the range of 50 - 200 G Ω this would mean that the *minimum* noise attributable to the seal is in the range of 0.03 - 0.06 pA rms in a 10 kHz bandwidth. Recent data suggests that under favorable circumstances seal noise may be as low as these predicted values. However, experience indicates that there is a good deal of variability in the noise of patches even when the seal resistances are very high and all other precautions necessary to minimize noise have been strictly observed. Some of this variability may well arise from the seal.

Limits of Patch-Clamp Noise Performance

With a capacitive-feedback headstage, such as the CV 201A or CV 202A of the Axopatch 200A, whose open circuit noise is less than 0.16 pA rms in a 10 kHz bandwidth, the best total noise performance obtained in an actual recording is \approx 0.09 pA rms in a 5 kHz bandwidth and \approx 0.19 pA rms in a bandwidth of 10 kHz (all bandwidths are the -3 dB frequency of an 8-pole Bessel filter). For both bandwidths the headstage by itself accounts for approximately 50% of the total noise and the holder, pipette and seal account for the other 50% of the total. Thus if the headstage was somehow reduced to zero, the total noise for such a patch would fall to about 0.13 - 0.14 pA rms in a 10 kHz bandwidth. It seems reasonable to expect that further improvements in the noise associated with the holder and pipette can be expected in the future. Of course, the noise associated with the seal is a fundamental limitation of the patch clamp technique. An absolute minimum estimate for seal noise in a 10 kHz bandwidth is about 0.03 - 0.04 pA rms; this assumes a 100 - 200 G Ω seal producing only thermal noise. An estimate of the minimum noise associated with an improved holder, quartz pipette and seal in a 10 kHz bandwidth is then about 0.06 pA rms. These figures suggest that as holder and pipette technology continues to improve, it will be worthwhile to continue to seek methods to reduce the noise of the headstage itself. It is reasonable to expect that total noise levels roughly half of the



best values achieved to date will become possible. However, to achieve such noise levels, careful attention to every aspect of the patch-clamp technique will be important.

Further Reading

Rae, J.L., Levis, R.A. *A method for exceptionally low noise single-channel recording.* Pflügers Arch. 420, 618-620, 1992.

Rae, J.L., Levis, R.A. *Quartz pipettes for single-channel recording.* Biophys. 64, A201 (P394), 1993.

Sakmann, B. and Neher, E., Eds. **Single-Channel Recording.** New York: Plenum Press, 1983.



